Synthesis and characterisation of mono- and di-nuclear mixed phosphathia complexes of gold(I): crystal structures of [Au(RSC$_2$H$_4$SR)]PF$_6$, [Au(RSC$_3$H$_6$SR)]PF$_6$ and [Au$_2$(RSC$_2$H$_4$SR)$_2$]Cl$_2$·4CH$_2$Cl$_2$ (R = Ph$_2$PC$_2$H$_4$)
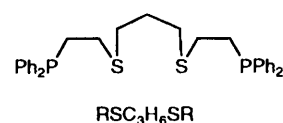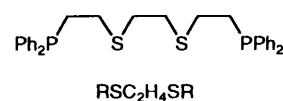
Alexander M. Gibson and Gillian Reid *

Department of Chemistry, University of Southampton, Highfield, Southampton SO17 1BJ, UK

Mononuclear gold(I) complexes of two linear P$_2$S$_2$ donor ligands, [AuL]PF$_6$ [L = RSC$_2$H$_4$SR or RSC$_3$H$_6$SR (R = Ph$_2$PC$_2$H$_4$)] have been prepared by reaction of [AuCl(tht)] (tht = tetrahydrothiophene) with L and TlPF$_6$ in MeCN solution. The crystal structure of [Au(RSC$_2$H$_4$SR)]$^+$ shows a primary P$_2$-donor set with additional long-range thioether interactions giving a distorted linear geometry around Au^I in the solid state; Au–P 2.284(7), 2.302(7), Au · · · S 2.899(6), 3.190(7) Å. The structure of [Au(RSC$_3$H$_6$SR)]$^+$ shows a very similar arrangement; Au–P 2.279(6), 2.287(6) Å, Au · · · S 3.097(5), 3.101(6) Å. The non-conducting binuclear species [Au$_2$Cl$_2$L] were obtained by reaction of [AuCl(tht)] with L in a 2:1 molar ratio in CH$_2$Cl$_2$ solution, while a 1:1 [AuCl(tht)]: RSC$_2$H$_4$SR ratio yielded the unusual species [Au$_2$(RSC$_2$H$_4$SR)$_2$]Cl$_2$, the crystal structure of which shows a linear P$_2$-donor set at each Au, giving a helical cavity which contains a Cl$^-$ anion. All complexes have been characterised by IR, ^{1}H and ^{31}P NMR spectroscopies, FAB mass spectrometry and microanalyses.

Gold–phosphine chemistry has attracted considerable attention in recent years since the antitumour activity of complexes such as [Au(L–L)$_2$]$^+$ (L–L = diphosphine) was noted.[1] Mixed phosphine–thiolate complexes such as [Au(SR)(PEt$_3$)] are also important in the treatment of arthritis.[2] In contrast to the vast number of gold(I)–phosphine complexes, very few examples of gold(I)–thioether complexes have been reported.[3,4] Schröder and co-workers[4] have shown that co-ordination of gold to homoleptic macrocyclic thioethers leads to highly unusual structural and electrochemical features. For example, all three mononuclear complex cations in the redox series [Au([9]aneS$_3$)$_2$]$^{+/2+/3+}$ ([9]aneS$_3$ = 1,4,7-trithiacyclonon-ane) have been isolated and structurally characterised. A feature common to the gold(I)–thioether macrocyclic complexes is the occurrence of long-range weak Au · · · S interactions of *ca.* 3 Å. To our knowledge interactions of this type have not been observed for acyclic thioethers on Au^I.

As part of a study on the relative co-ordinating abilities of phosphine *vs.* thioether donors, we have been investigating the co-ordination chemistry of mixed phosphathia macrocycles *e.g.* Ph$_2$[14]aneP$_2$S$_2$[5] (4,8-diphenyl-1,11-dithia-4,8-diphospha-cyclotetradecane) and their open-chain analogues RSC$_2$H$_4$SR and RSC$_3$H$_6$SR (R = Ph$_2$PC$_2$H$_4$) with transition-metal ions. We have shown that RSC$_2$H$_4$SR co-ordinates readily to metal ions which have a strong preference for six-co-ordination, such as Ru^{II}, Rh^{III} and Ir^{III}, to give complexes of the form [Ru(RSC$_2$-H$_4$SR)Cl$_2$] and [M(RSC$_2$H$_4$SR)Cl$_2$]$^+$ (M = Rh or Ir), as single isomers in which the Cl$^-$ ligands occupy mutually *cis* co-ordination sites, with the phosphathia ligand co-ordinated in a manner which leaves the phosphine functions mutually *trans* and the thioether functions *trans* to Cl.[6] The compound RSC$_2$H$_4$SR co-ordinates tetrahedrally with the d^{10} ions Cu^I and Ag^I *via* all four donor atoms.[7] Whereas Cu^I shows a preference for tetrahedral co-ordination, Au^I usually shows a strong preference for linear, two-co-ordinate geometries. We were therefore interested to establish the effects of the mismatch between the preference of the gold(I) centre and the potentially tetradentate P$_2$S$_2$ donor ligands. We now report the syntheses of the mononuclear species [AuL]PF$_6$, the neutral binuclear species [Au$_2$Cl$_2$L] (L = RSC$_2$H$_4$SR or RSC$_3$H$_6$SR) and the cationic binuclear species [Au$_2$(RSC$_2$H$_4$SR)$_2$]Cl$_2$, together

RSC$_2$H$_4$SR

RSC$_3$H$_6$SR

with the single-crystal structures of [Au(RSC$_2$H$_4$SR)]PF$_6$, [Au(RSC$_3$H$_6$SR)]PF$_6$ and [Au$_2$(RSC$_2$H$_4$SR)$_2$]Cl$_2$·4CH$_2$Cl$_2$.

Results and Discussion

Reaction of [AuCl(tht)] (tht = tetrahydrothiophene) with 1 molar equivalent of L (RSC$_2$H$_4$SR or RSC$_3$H$_6$SR) in degassed MeCN solution gives a colourless solution. Addition of 1 molar equivalent of TlPF$_6$ gives a white precipitate of TlCl after a few minutes. After filtering to remove this, addition of diethyl ether affords a white solid in each case which can be isolated by filtration and dried *in vacuo*. It is important to have L in solution with the [AuCl(tht)] for a few minutes prior to adding the TlPF$_6$, otherwise gold mirrors tend to be produced. The FAB mass spectra of these apparently air- and light-stable products show highest mass peaks at m/z = 715 and 729, consistent with [AuL]$^+$ (L = RSC$_2$H$_4$SR and RSC$_3$H$_6$SR respectively). Other peaks corresponding to fragmentation products are also observed. The IR spectra show peaks due to the PF$_6^-$ anions and ligand. Together with ^{1}H NMR spectroscopic and microanalytical data, these results indicate the formulation [AuL]PF$_6$ for the products. At 300 K the ^{31}P-{^{1}H} NMR spectrum of [Au(RSC$_2$H$_4$SR)]PF$_6$ shows a singlet at δ 32.9 due to co-ordinated L (free L, δ −16.3), and a septet at δ −146.0 due to PF$_6^-$ anion. These resonances do not shift on cooling to 200 K, suggesting on average, P$_2$ co-ordination at Au^I in solution within the temperature range studied. Similarly, the ^{31}P-{^{1}H} NMR spectrum (145.8 MHz, CH$_2$Cl$_2$–CDCl$_3$) of [Au(RSC$_3$H$_6$SR)]PF$_6$ shows a singlet at δ 29.8 due to L (free L,

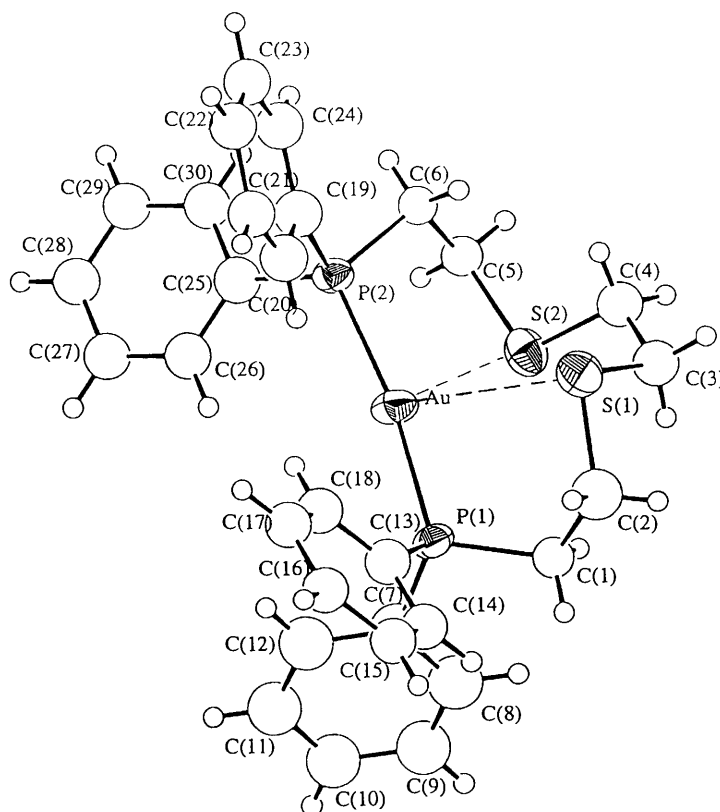**Fig. 1** View of the structure of the $[Au(RSC_2H_4SR)]^+$ cation with the numbering scheme adopted. Ellipsoids are drawn at 40% probability

Table 1 Selected bond lengths (Å) and angles (°) for $[Au(RSC_2H_4SR)]^+$

Au–P(1)	2.284(7)	Au–P(2)	2.302(7)
Au $\cdots$ S(1)	3.190(7)	Au $\cdots$ S(2)	2.899(6)
S(1)–C(2)	1.92(3)	S(1)–C(3)	1.87(3)
S(2)–C(4)	1.86(2)	S(2)–C(5)	1.86(3)
P(1)–C(1)	1.83(2)	P(1)–C(7)	1.79(2)
P(1)–C(13)	1.79(2)	P(2)–C(6)	1.88(2)
P(2)–C(19)	1.81(2)	P(2)–C(25)	1.81(2)
C(1)–C(2)	1.52(4)	C(3)–C(4)	1.47(4)
C(5)–C(6)	1.54(3)		
P(1)–Au–P(2)	169.1(2)	C(2)–S(1)–C(3)	100(1)
C(4)–S(2)–C(5)	103(1)	Au–P(1)–C(1)	114.1(8)
Au–P(1)–C(7)	114.2(7)	Au–P(1)–C(13)	111.7(6)
C(1)–P(1)–C(7)	104(1)	C(1)–P(1)–C(13)	106.8(10)
C(7)–P(1)–C(13)	105.2(8)	Au–P(2)–C(6)	109.1(8)
Au–P(2)–C(19)	113.6(6)	Au–P(2)–C(25)	115.7(6)
C(6)–P(2)–C(19)	105.2(9)	C(6)–P(2)–C(25)	107.9(9)
C(19)–P(2)–C(25)	104.7(8)	P(1)–C(1)–C(2)	112(1)
S(1)–C(2)–C(1)	113(1)	S(1)–C(3)–C(4)	111(1)
S(2)–C(4)–C(3)	112(1)	S(2)–C(5)–C(6)	113(1)
P(2)–C(6)–C(5)	110(1)		

δ — 16.3) and a septet at δ — 146.1 (PF_6^-) at 300 K, which do not shift upon cooling.

In order to establish the stereochemistries at Au^I and to determine whether the thioether donors interact with the metal ion in the solid state, single-crystal structure analyses on $[AuL]PF_6$ were undertaken. For L = RSC_2H_4SR the crystal structure shows (Fig. 1, Table 1) discrete $[Au(RSC_2H_4SR)]^+$ cations and PF_6^- anions. In the cation both P donors are co-ordinated to the gold(I) centre, Au–P(1) 2.284(7) and Au–P(2) 2.302(7) Å, with a P(1)–Au–P(2) angle of 169.1(2)°. Additionally, both thioether donors are involved in long-range, weak interactions, Au $\cdots$ S(1) 3.190(7) and Au $\cdots$ S(2) 2.899(6) Å. The other angles around the metal centre, S(1)–Au–S(2) 70.6(2), S(1)–Au–P(1) 76.0(2), S(2)–Au–P(2) 82.6(2), S(1)–Au–P(2)

109.2(2) and S(2)–Au–P(1) 108.5(3)°, indicate a geometry at Au^I distorted from linear towards tetrahedral, with primary P_2 and secondary S_2 co-ordination.

The crystal structure of $[Au(RSC_3H_6SR)]PF_6$ shows (Fig. 2, Table 2) very similar features, with Au–P(1) 2.279(6) and Au–P(2) 2.287(6) Å in the primary co-ordination set, and long-range gold–thioether interactions, Au $\cdots$ S(1) 3.097(5) and Au $\cdots$ S(2) 3.101(6) Å. In this case the P(1)–Au–P(2) angle is 158.9(2)°, a greater deviation from linearity than that for $[Au(RSC_2H_4SR)]^+$ which may be a consequence of the steric requirements of the additional CH_2 unit linking the S-donors. The other angles around the gold(I) centre are: S(1)–Au–S(2) 76.2(2), S(1)–Au–P(1) 78.1(2), S(2)–Au–P(2) 77.6(2), S(1)–Au–P(2) 113.7(2) and S(2)–Au–P(1) 123.2(2)°. These structures contrast with that seen previously for [Cu(RS-C_2H_4SR)]PF_6, which shows genuine tetrahedral P_2S_2 co-ordination at Cu^I, Cu–P 2.233(2), 2.242(2), Cu–S 2.367(2), 2.385(2) Å.[7] The newly synthesised mononuclear gold complexes appear to adopt structures which are a compromise between the linear co-ordination preferred by Au^I and the four-co-ordination favoured by the potentially tetradentate phosphathia ligands. The Au $\cdots$ S interactions in $[AuL]^+$ are comparable with those observed in the gold(I)–thioether macrocyclic complexes which show similar [2 + 2] co-ordination; e.g. in $[Au([18]aneS_6)]^+$ ($[18]aneS_6$ = 1,4,7,10,13,16–hexathia-cyclooctadecane) Au–S 2.321(3), 2.320(4), Au $\cdots$ S 2.856(4), 2.870(4) Å and in $[Au([15]aneS_5)]^+$ ($[15]aneS_5$ = 1,4,7,10,13-pentathiacyclopentadecane) Au–S 2.300(1), 2.293(1), Au $\cdots$ S 3.209(1), 3.106(1) Å.[4] Linear P_2-donor co-ordination at Au^I has been observed in several systems, for example $[Au(PPh_2-Me)_2]^+$ [8] and $[Au\{P(C_6H_{11})_3\}_2]^+$.[9] These exhibit similar Au–P bond lengths to those observed in the phosphathia complexes described here [Au–P 2.316(4) and 2.305(average) Å, respectively].

Cyclic voltammetry on $[Au(RSC_2H_4SR)]PF_6$ recorded in MeCN solution (0.1 mol dm^{-3} $NBu^n_4BF_4$ supporting electrolyte) shows an irreversible oxidation at +0.82 V vs. ferrocene–ferrocenium. Similarly, $[Au(RSC_3H_6SR_3)]PF_6$
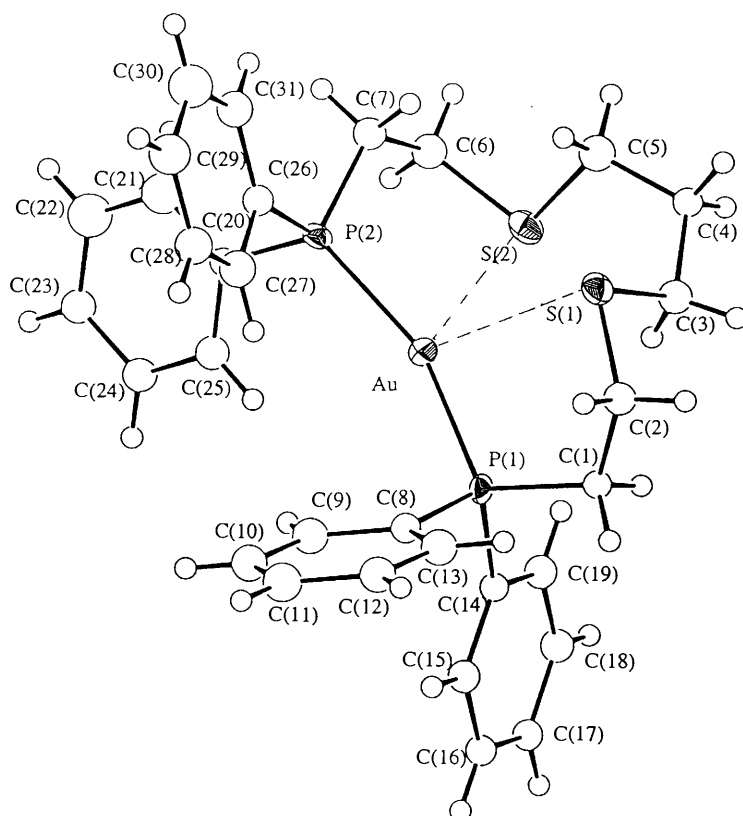
Fig. 2 View of the structure of the [Au(RSC$_3$H$_6$SR)]$^+$ cation with the numbering scheme adopted. Ellipsoids are drawn at 40% probability

Table 2 Selected bond lengths (Å) and angles (°) for [Au(RS-C$_3$H$_6$SR)]$^+$

Au–P(1)	2.279(6)	Au–P(2)	2.287(6)
Au···S(1)	3.097(5)	Au···S(2)	3.101(6)
S(1)–C(2)	1.79(2)	S(1)–C(3)	1.83(2)
S(2)–C(5)	1.86(2)	S(2)–C(6)	1.80(2)
P(1)–C(1)	1.81(2)	P(1)–C(14)	1.824(10)
P(1)–C(8)	1.82(1)	P(2)–C(7)	1.80(2)
P(2)–C(26)	1.84(1)	P(2)–C(20)	1.81(1)
C(1)–C(2)	1.54(2)	C(3)–C(4)	1.52(3)
C(4)–C(5)	1.53(3)	C(6)–C(7)	1.56(3)
P(1)–Au–P(2)	158.9(2)	C(2)–S(1)–C(3)	98.9(10)
C(5)–S(2)–C(6)	100.0(10)	Au–P(1)–C(1)	115.5(7)
Au–P(1)–C(14)	120.5(5)	Au–P(1)–C(8)	107.0(5)
C(1)–P(1)–C(14)	98.8(7)	C(1)–P(1)–C(8)	107.7(8)
C(1)–P(1)–C(8)	106.5(6)	Au–P(2)–C(7)	113.3(8)
Au–P(2)–C(26)	112.4(5)	Au–P(2)–C(20)	116.4(4)
C(7)–P(2)–C(26)	106.0(8)	C(7)–P(2)–C(20)	104.0(9)
C(26)–P(2)–C(20)	103.6(7)	P(2)–C(7)–C(6)	113(1)
P(1)–C(1)–C(2)	114(1)	S(1)–C(2)–C(1)	116(1)
S(1)–C(3)–C(4)	110(1)	C(3)–C(4)–C(5)	115(1)
S(2)–C(5)–C(4)	110(1)	S(2)–C(6)–C(7)	113(1)

shows an irreversible oxidation at +0.91 V. These are tentatively assigned to Au^I–Au^{III} processes. These oxidation potentials are considerably more anodic compared to the Au^I–Au^{II} couples for thioether macrocyclic complexes, e.g. for [Au([18]aneS$_6$)]$^{+/2+}$ $E_{\frac{1}{2}}$ = +0.36 V, probably reflecting the softer nature of the phosphine functions relative to the thioether functions.[4]

In the absence of TlPF$_6$, RSC$_2$H$_4$SR and RSC$_3$H$_6$SR also react with 2 molar equivalents of [AuCl(tht)] in MeCN solution to give, upon reduction of the volume of solvent and addition of diethyl ether, the binuclear species [Au$_2$Cl$_2$L] as stable white solids. These compounds are non-electrolytes in CH$_2$Cl$_2$ solution. The IR spectra each show a single Au–Cl stretching vibration, ν(Au–Cl) 324 and 326 cm^{-1}, respectively, confirming the presence of a terminal Cl$^-$ ligand on gold(I), and

FAB mass spectrometry (3-nitrobenzyl alcohol matrix) shows peaks corresponding to [Au$_2$^{35}Cl(L)]$^+$ (m/z = 947, 961), as well as several lower-mass peaks corresponding to fragmentation products through loss of Cl and Au atoms. The ^{31}P-{^{1}H} NMR spectra (145.8 MHz, CH$_2$Cl$_2$–CDCl$_3$, 300 K) show a singlet in each case at δ +25.3 and +24.9 respectively. These resonances are unaffected by cooling to 200 K and are upfield relative to those observed for [AuL]PF$_6$, which involve mainly P$_2$ co-ordination in the solid state and probably in solution. The related binuclear species [Au$_2$Cl$_2$(dppe)] (dppe = Ph$_2$PCH$_2$CH$_2$PPh$_2$), which involves two gold(I) ions each co-ordinated to a linear PCl donor set, shows a singlet at δ +31.5 in the ^{31}P NMR spectrum.[10] It seems likely that the complexes [Au$_2$Cl$_2$L] also involve PCl co-ordination at Au^I, with the thioether donors probably not co-ordinating in solution. Comparison of the chemical shift for the homoleptic phosphine complex [Au(dppe)$_2$]$^+$ with our new complexes [AuL]$^+$ is not possible since [Au(dppe)$_2$]$^+$ is a genuinely four-co-ordinate cation.[10]

Surprisingly, a 1:1 molar ratio of [AuCl(tht)] and RSC$_2$H$_4$SR reacts in CH$_2$Cl$_2$ solution, to give, upon addition of diethyl ether, an air-stable white solid of very different composition. Importantly in this case, the IR spectrum of the isolated solid shows no Au–Cl stretching vibration in the range 200–400 cm^{-1}. This contrasts with the products [Au$_2$Cl$_2$L] described above, which show very distinctive terminal Au–Cl stretches. The FAB mass spectrum of the product (3-nitrobenzyl alcohol matrix) reveals the highest-mass peak at m/z = 715, consistent with [^{197}Au(RSC$_2$H$_4$SR)]$^+$, as well as peaks with lower m/z corresponding to fragmentation products. Importantly, there is no evidence for Cl-containing species in the mass spectrum. Microanalyses on the bulk sample isolated are consistent with the formulation [Au$_2$(RSC$_2$H$_4$SR)$_2$]Cl$_2$. Single crystals of the product [Au$_2$(RSC$_2$H$_4$SR)$_2$]Cl$_2$·4CH$_2$Cl$_2$ were obtained by layering a CH$_2$Cl$_2$ solution of the complex with pentane at −15 °C. The X-ray analysis shows (Fig. 3, Table 3) a very unexpected and unusual structure comprising binuclear [Au$_2$(RSC$_2$H$_4$SR)$_2$]$^{2+}$ cations with crystallographic C_2 symmetry, with a Cl$^-$ anion occupying this two-fold site

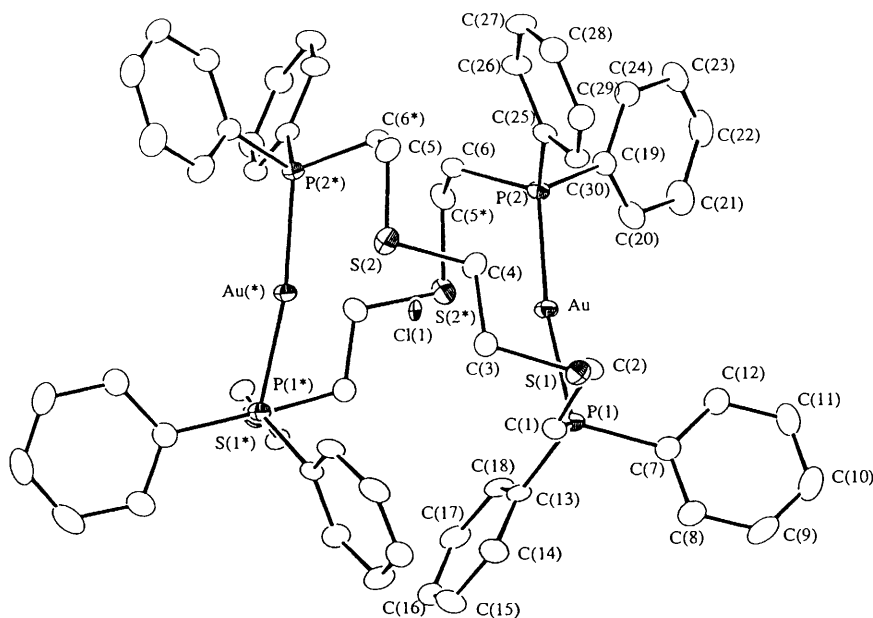**Fig. 3** View of the structure of $[Au_2(RSC_2H_4SR)_2]^{2+}$ showing the trapped Cl^- ion $[Cl(1)]$ and the numbering scheme adopted (H atoms are omitted for clarity and atoms marked with an asterisk are related to the non-asterisked ones by a C_2 operation)

Table 3 Selected bond lengths (Å) and angles (°) for $[Au_2(RSC_2H_4SR)_2]^{2+}$

Au–P(1)	2.304(2)	Au–P(2)	2.316(2)
S(1)–C(2)	1.814(6)	S(1)–C(3)	1.801(6)
S(2)–C(4)	1.794(6)	S(2)–C(5)	1.806(7)
P(1)–C(1)	1.820(6)	P(1)–C(7)	1.834(6)
P(1)–C(13)	1.829(6)	P(2)–C(6)	1.819(6)
P(2)–C(19)	1.815(6)	P(2)–C(25)	1.814(6)
C(1)–C(2)	1.515(8)	C(3)–C(4)	1.528(9)
C(5)–C(6)	1.525(8)		
P(1)–Au–P(2)	169.96(6)	C(2)–S(1)–C(3)	101.4(3)
C(4)–S(2)–C(5)	99.1(3)	Au–P(1)–C(1)	108.7(2)
Au–P(1)–C(7)	115.6(2)	Au–P(1)–C(13)	115.3(2)
C(1)–P(1)–C(7)	104.2(3)	C(1)–P(1)–C(13)	104.9(3)
C(7)–P(1)–C(13)	107.2(3)	Au–P(2)–C(6)	112.9(2)
Au–P(2)–C(19)	112.7(2)	Au–P(2)–C(25)	113.4(2)
C(6)–P(2)–C(19)	104.1(3)	C(6)–P(2)–C(25)	104.0(3)
C(19)–P(2)–C(25)	109.0(3)	P(1)–C(1)–C(2)	110.4(4)
S(1)–C(2)–C(1)	113.7(4)	S(1)–C(3)–C(4)	113.9(4)
S(2)–C(4)–C(3)	109.3(4)	S(2)–C(5)–C(6)	114.7(5)
P(2)–C(6)–C(5)	114.0(4)	P(1)–C(7)–C(8)	121.2(5)
P(1)–C(7)–C(12)	119.2(5)	P(1)–C(13)–C(14)	122.1(5)
P(1)–C(13)–C(18)	119.2(5)	P(2)–C(19)–C(20)	117.8(5)
P(2)–C(19)–C(24)	123.4(5)	P(2)–C(25)–C(26)	122.7(5)
P(2)–C(25)–C(30)	118.8(5)		

$(0, y, 0.25)$, and in the centre of the metallocyclic cavity. A second Cl^- anion occupies another two-fold site $(0.5, y, 0.25)$. Four CH_2Cl_2 molecules were also found to be associated with each binuclear cation. The ligation at each gold(I) centre in this cationic species is approximately linear $[P(1)–Au(1)–P(2)$ $169.96(6)°]$ via one P-donor of two different bridging ligands, Au(1)–P(1) 2.304(2) and Au(1)–P(2) 2.316(2) Å. Surprisingly, although only co-ordinated to each Au^I by a single P-donor (the thioether donors are considered to be non-interacting in this case since the $Au \cdots S$ distances are 3.43 and 5.41 Å; significantly longer than the sum of the formal ionic radii of 1.37 + 1.84 = 3.21 Å for Au–S), the two bridging ligands link the metals in a helical manner. Furthermore, one of the Cl^- anions, $Cl(1)$, occupies the centre of the metallocyclic cavity, 2.8238(3) Å from each Au atom. These distances should probably be considered as weak $Au \cdots Cl \cdots Au$ interactions.

Wild and co-workers[11] have reported the crystal structure of a helical binuclear silver(I) complex, $[Ag_2L_2'][BF_4]_2$, $[L' = (S,S)-(+)-Ph_2PCH_2CH_2PPhCH_2CH_2PPhCH_2CH_2PPh_2$, a tetraphosphine analogue of $RSC_2H_4SR]$. In contrast to the structure observed for $[Au_2(RSC_2H_4SR)_2]Cl_2$, where the twisted conformation is apparently determined by the torsion angles in the ligands, each silver(I) centre in $[Ag_2L_2'][BF_4]_2$ is tetrahedrally co-ordinated via two P-donors of each L' ligand.

The $^{31}P-\{^1H\}$ NMR spectroscopic studies on $[Au_2(RS-C_2H_4SR)_2]Cl_2$ (145.8 MHz, $CH_2Cl_2–CDCl_3$) show a single resonance at δ +33.0, which is unaffected upon cooling from 300 to 200 K. This value is very similar to that observed for $[Au(RSC_2H_4SR)]PF_6$ and is consistent with retention of the P_2 donor set at each Au^I in solution. Assuming the formulation $[Au_2(RSC_2H_4SR)_2]Cl_2$, conductivity measurements indicate that this compound is a 1 : 1 electrolyte in CH_2Cl_2 and $MeNO_2$ solution.[12] Further work is underway to try to establish whether the Cl^- ion is retained within the cavity in certain solutions and, if so, whether it can be exchanged for other anions such as Br^-, SCN^-, CN^- and N_3^-. We are also trying to determine whether similar helical structural motifs occur in complexes with other P_2E_2-donor open-chain ligands (E = S, Se, O or NR).

Experimental

Infrared spectra were measured as KBr or CsI discs or as Nujol mulls using a Perkin-Elmer 983 spectrometer over the range 200–4000 cm^{-1}. Mass spectra were run by electron impact or fast-atom bombardment (FAB) using 3-nitrobenzyl alcohol as matrix on a VG Analytical 70-250-SE normal-geometry double-focusing spectrometer, ^1H NMR spectra using a Bruker AM300 spectrometer and ^{31}P NMR spectra using a Bruker AM360 spectrometer operating at 145.8 MHz and referenced to 85% H_3PO_4 (δ 0). Microanalyses were performed by the Imperial College microanalytical service. Cyclic voltammetric experiments were performed using an EG&G Princeton Applied Research model 362 scanning potentiostat with 0.1 mol dm^{-3} $NBu^n_4BF_4$ supporting electrolyte, using a double platinum electrode as working and auxiliary electrode and a Ag–AgCl reference electrode. All potentials are quoted versus ferrocene–ferrocenium. Conductivity measurements used a Pye conductance bridge and 0.001 mol dm^{-3} solutions of the complexes in CH_2Cl_2 or $MeNO_2$. The compounds $AuCl(tht)^{13}$ and

Table 4 Crystallographic data collection and refinement parameters *

	[Au(RSC$_2$H$_4$SR)]PF$_6$	[Au(RSC$_3$H$_6$SR)]PF$_6$	[Au$_2$(RSC$_2$H$_4$SR)$_2$]Cl$_2$·4CH$_2$Cl$_2$
Formula	C$_{30}$H$_{32}$AuF$_6$P$_3$S$_2$	C$_{31}$H$_{34}$AuF$_6$P$_3$S$_2$	C$_{60}$H$_{68}$Au$_2$Cl$_2$P$_4$S$_4$·4CH$_2$Cl$_2$
M	860.6	874.6	1841.9
Colour, morphology	Colourless, tablet	Colourless, block	Colourless, column
Crystal dimensions/mm	0.35 × 0.15 × 0.10	0.40 × 0.20 × 0.10	0.90 × 0.30 × 0.20
Crystal system	Orthorhombic	Monoclinic	Monoclinic
Space group	$Pna2_1$	$P2_1/n$	$C2/c$
a/Å	13.071(3)	13.304(4)	21.736(3)
b/Å	19.159(1)	15.290(3)	16.615(4)
c/Å	12.925(2)	16.460(3)	21.140(3)
β/°		105.33(2)	106.902(8)
U/Å^3	3237.0(8)	3229(1)	7304(1)
$F(000)$	1688	1720	3632
D_c/g cm^{-3}	1.766	1.799	1.675
μ(Mo-Kα)/cm^{-1}	48.54	49.06	46.31
ω Scan width/°	0.79 + 0.35 tan θ	1.37 + 0.35 tan θ	1.37 + 0.35 tan θ
Maximum, minimum transmission factors	1.000, 0.770	1.000, 0.472	1.000, 0.575
hkl Octants explored	0–14, 0–22, 0–15	0–16, 0–18, −20 to 20	0–25, 0–18, −24 to 23
Unique observed reflections	3238	5923	6678
R_{int} (based on F^2)	—	0.148	0.071
Observed reflections	1535	2261	5183
$[I_o > n\sigma(I_o)]$	(n = 2)	(n = 2)	(n = 2.5)
No. parameters	161	185	381
Goodness of fit	1.91	1.74	2.63
R	0.047	0.059	0.033
R'	0.043	0.053	0.033
Final Δ/σ	0.00	0.02	0.00
Maximum, minimum residual peaks/e Å^{-3}	0.77, −1.08	2.20, −1.35	1.71, −1.76

* Details in common: Z = 4; $2\theta_{max}$ 50°.

Table 5 Fractional atomic coordinates for [Au(RSC$_2$H$_4$SR)]PF$_6$

Atom	x	y	z	Atom	x	y	z
Au	−0.126 35(8)	−0.193 98(1)	−0.012 1(6)	C(10)	−0.336(1)	−0.063 6(10)	−0.335(1)
S(1)	0.059 9(6)	−0.294 3(4)	0.045 7(6)	C(11)	−0.304(1)	−0.031 2(8)	0.244(2)
S(2)	−0.201 2(5)	−0.335 4(3)	0.013 4(7)	C(12)	−0.222(2)	−0.058(1)	0.188(1)
P(1)	−0.072 1(5)	−0.154 0(4)	0.145 1(5)	C(13)	0.020(1)	−0.085 6(7)	0.132(1)
P(2)	−0.172 7(5)	−0.213 3(3)	−0.181 5(5)	C(14)	0.083(1)	−0.069 7(8)	0.216(1)
P(3)	−0.660(1)	−0.118 4(7)	−0.568 3(9)	C(15)	0.159(1)	−0.019 0(9)	0.206(1)
F(1)	−0.682(2)	−0.133(1)	−0.450(1)	C(16)	0.171 9(10)	0.015 7(7)	0.112(1)
F(2)	−0.581(1)	−0.179(1)	−0.571(2)	C(17)	0.109(1)	−0.000 2(7)	0.028(1)
F(3)	−0.744(2)	−0.171(1)	−0.600(2)	C(18)	0.033(1)	−0.050 9(8)	0.038(1)
F(4)	−0.640(1)	−0.105(1)	−0.684(1)	C(19)	−0.078(1)	−0.185 4(9)	−0.274(1)
F(5)	−0.743(1)	−0.058 5(9)	−0.564(1)	C(20)	−0.005(1)	−0.136 5(9)	−0.242 1(10)
F(6)	−0.576(1)	−0.066(1)	−0.537(2)	C(21)	0.065(1)	−0.109 8(7)	−0.313(1)
C(1)	−0.014(2)	−0.221(1)	0.227(2)	C(22)	0.063(1)	−0.132 1(9)	−0.416(1)
C(2)	0.082(2)	−0.252(1)	0.179(2)	C(23)	−0.009(1)	−0.181 0(8)	−0.447 6(10)
C(3)	−0.009(2)	−0.376(1)	0.085(2)	C(24)	−0.080(1)	−0.207 6(7)	−0.377(1)
C(4)	−0.088(2)	−0.394(1)	0.009(3)	C(25)	−0.289(1)	−0.171 4(8)	−0.223(1)
C(5)	−0.256(2)	−0.342(1)	−0.119(2)	C(26)	−0.323(1)	−0.112 1(9)	−0.170(1)
C(6)	−0.187(2)	−0.310(1)	−0.203(2)	C(27)	−0.404(1)	−0.073 1(7)	−0.210(1)
C(7)	−0.172(1)	−0.118(1)	0.224(2)	C(28)	−0.452 1(10)	−0.093 4(8)	−0.301(1)
C(8)	−0.204(1)	−0.150 6(8)	0.315(2)	C(29)	−0.418(1)	−0.152 8(9)	−0.354(1)
C(9)	−0.286(1)	−0.123 3(10)	0.370(1)	C(30)	−0.337(1)	−0.191 7(7)	−0.315(1)

RSC$_3$H$_6$SR [14] were prepared by the literature methods, RSC$_2$H$_4$SR by a slight modification of that for the latter.

Syntheses

(a) **[Au(RSC$_2$H$_4$SR)]PF$_6$.** To a solution of RSC$_2$H$_4$SR (100 mg, 0.192 mmol) in degassed MeCN (20 cm^3) was added [AuCl(tht)] (62 mg, 0.192 mmol) in one portion. The resulting mixture was stirred for 15 min, then TlPF$_6$ (68 mg, 0.192 mmol) was added and the mixture stirred overnight. The TlCl was filtered off and the filtrate reduced in volume (2 cm^3) *in vacuo*. Addition of Et$_2$O (10 cm^3) afforded a white microcrystalline solid (yield: 98 mg, 60%) (Found: C, 41.6; H, 3.8. C$_{30}$H$_{32}$AuF$_6$P$_3$S$_2$ requires C, 41.9; H, 3.7%). FAB mass spectrum: m/z = 715, 529 and 441; calc. 715 for [Au-(RSC$_2$H$_4$SR)]$^+$, 530 for [Au{Ph$_2$P(CH$_2$)$_2$S(CH$_2$)$_2$S(C-H$_2$)$_2$}]$^+$ and 441 for [Au{Ph$_2$P(CH$_2$)$_2$S}]$^+$. NMR (300 K): ^{31}P-{^{1}H} (145.8 MHz, CH$_2$Cl$_2$–CDCl$_3$), δ 32.9 (s, 2 P, RSC$_2$H$_4$SR) and −146.0 (spt, 1 P, PF$_6$$^-$); ^{1}H (300 MHz, CDCl$_3$), δ 7.80–7.35 (m, 20 H, Ph), 2.96–2.82 (m, 12 H, CH$_2$). IR (KBr disc): 2913m, 1985w, 1821w, 1585w, 1481m, 1434s, 1309w, 1255w, 1185w, 1102m, 1083w, 1026w, 998w, 873vs, 742m, 692s, 557s, 516m, 491m, 432w and 347vw cm^{-1}.

(b) **[Au(RSC$_3$H$_6$SR)]PF$_6$.** As (a) except using RSC$_3$H$_6$SR (60 mg, 0.113 mmol), [AuCl(tht)] (38 mg, 0.113 mmol) and TlPF$_6$ (40 mg, 0.113 mmol) in degassed MeCN (20 cm^3). Addition of Et$_2$O (20 cm^3) yielded a white solid (60 mg, 60%) (Found: C, 39.1; H, 3.4. C$_{31}$H$_{34}$AuF$_6$P$_3$S$_2$· CH$_2$Cl$_2$ requires C, 38.8; H,

Table 6 Fractional atomic coordinates for [Au(RSC₃H₆SR)]PF₆

Table 6 Fractional atomic coordinates for $[Au(RSC_3H_6SR)]PF_6$

Atom	x	y	z	Atom	x	y	z
Au	0.238 60(7)	0.108 69(7)	0.555 94(6)	C(11)	0.296(1)	−0.166 2(9)	0.342 8(7)
S(1)	0.047 7(4)	0.026 7(4)	0.601 6(4)	C(12)	0.240 4(9)	−0.204 0(7)	0.394 6(9)
S(2)	0.187 4(4)	0.240 7(4)	0.682 3(4)	C(13)	0.240 0(9)	−0.164 3(8)	0.470 9(8)
P(1)	0.295 1(4)	−0.030 2(4)	0.592 1(4)	C(14)	0.422 6(7)	−0.049 4(9)	0.665 1(7)
P(2)	0.200 0(4)	0.233 1(4)	0.476 7(4)	C(15)	0.492 9(9)	−0.110 2(9)	0.648 6(6)
P(3)	0.304 5(4)	0.098 0(5)	0.945 6(4)	C(16)	0.586 8(8)	−0.126 3(8)	0.708 7(8)
F(1)	0.377(1)	0.024(1)	0.986(1)	C(17)	0.610 4(7)	−0.081 5(8)	0.785 3(7)
F(2)	0.352(1)	0.106(2)	0.869(1)	C(18)	0.540 2(9)	−0.020 6(8)	0.801 7(7)
F(3)	0.223(1)	0.171(1)	0.905(1)	C(19)	0.446 3(8)	−0.004 6(8)	0.741 6(8)
F(4)	0.249(1)	0.090(1)	1.018 2(10)	C(20)	0.310 0(8)	0.295 7(9)	0.462 7(9)
F(5)	0.379 5(9)	0.166 9(10)	1.001(1)	C(21)	0.297 8(7)	0.379 0(9)	0.426 7(9)
F(6)	0.227(1)	0.028 1(9)	0.892 9(9)	C(22)	0.385(1)	0.425 0(7)	0.417 5(9)
C(1)	0.216(1)	−0.093(1)	0.645(1)	C(23)	0.483 6(8)	0.387 9(9)	0.444 3(8)
C(2)	0.097(1)	−0.082(1)	0.609(1)	C(24)	0.495 9(7)	0.304 7(9)	0.480 3(9)
C(3)	0.090(1)	0.057(1)	0.713(1)	C(25)	0.409 1(10)	0.258 6(7)	0.489 5(9)
C(4)	0.036(1)	0.141(1)	0.728(1)	C(26)	0.123 0(9)	0.210 5(9)	0.368 1(7)
C(5)	0.047(2)	0.218(1)	0.672(1)	C(27)	0.145 6(8)	0.133 9(8)	0.330 4(8)
C(6)	0.175(2)	0.334(1)	0.613(1)	C(28)	0.089 5(10)	0.112 9(8)	0.248 5(8)
C(7)	0.126(1)	0.311(1)	0.519(1)	C(29)	0.010 9(10)	0.169(1)	0.204 2(6)
C(8)	0.295 4(10)	−0.087 0(8)	0.495 3(7)	C(30)	−0.011 7(9)	0.245 2(9)	0.241 9(9)
C(9)	0.351 1(9)	−0.049 3(7)	0.443 4(8)	C(31)	0.044 3(10)	0.266 2(7)	0.323 8(9)
C(10)	0.351 5(9)	−0.088 9(9)	0.367 1(8)				

3.7%). FAB mass spectrum: m/z = 729, 653, 543, 515 and 441; calc. 729 for $[Au(RSC_3H_6SR)]^+$, 652 for $[Au\{Ph_2P-(CH_2)_2S(CH_2)_3S(CH_2)_2PPh\}]^+$, 544 for $[Au\{Ph_2P(CH_2)_2-S(CH_2)_3S(CH_2)_2\}]^+$, 516 for $[Au\{Ph_2P(CH_2)_2S(CH_2)_3S\}]^+$ and 441 for $[Au\{Ph_2P(CH_2)_2S\}]^+$. NMR (300 K): $^{31}P-\{^1H\}$ (145.8 MHz, CH_2Cl_2–$CDCl_3$), δ 29.8 (s, 2 P, RSC_3H_6SR) and −146.1 (spt, 1 P, PF_6^-); ^1H (300 MHz, $CDCl_3$), δ 7.80–7.35 (m, 20 H, Ph), 3.05–2.73 (m, 12 H, CH_2) and 1.90 (t, 2 H, $CH_2CH_2CH_2$). IR (KBr disc): 2919m, 1971w, 1710w, 1535w, 1481w, 1433s, 1329w, 1260w, 1157m, 1101s, 1025w, 998w, 837vs, 742m, 693s, 557s, 516m and 490w cm⁻¹.

(c) **[Au₂(RSC₂H₄SR)Cl₂].** To a solution of RSC_2H_4SR (100 mg, 0.192 mmol) in degassed MeCN (30 cm³) was added [AuCl(tht)] (120 mg, 0.384 mmol) in one portion. The resulting mixture was stirred for 1 h, then reduced in volume (2 cm³) in vacuo. Addition of Et_2O (20 cm³) yielded a white solid (142 mg, 75%) (Found: C, 32.2; H, 2.8. $C_{30}H_{32}Au_2Cl_2P_2S_2$·2CHCl₃ requires C, 32.4; H, 2.8%). FAB mass spectrum: m/z = 947, 910 and 715; calc. 947 for $[Au_2(RSC_2H_4SR)^{35}Cl]$, 912 for $[Au_2(RSC_2H_4SR)]$ and 715 for $[Au(RSC_2H_4SR)]$. NMR (300 K): $^{31}P-\{^1H\}$ (145.8 MHz, CH_2Cl_2–$CDCl_3$), δ 25.3 (s); ^1H (300 MHz, $CDCl_3$), δ 7.80–7.45 (m, 20 H, Ph) and 2.95–2.70 (m, 12 H, CH_2). IR (CsI disc): 2962m, 2904m, 1963w, 1894w, 1814w, 1584w, 1481m, 1432s, 1332w, 1309m, 1260w, 1183w, 1157m, 1103s, 1025w, 997w, 803vw, 744m, 692m, 521m, 486w and 324w cm⁻¹. Conductivity measurement (CH_2Cl_2 solution): non-electrolyte.

(d) **[Au₂(RSC₃H₆SR)Cl₂].** As for (c) except using RSC_3H_6SR (40 mg, 0.075 mmol) and [AuCl(tht)] (51 mg, 0.15 mmol) in MeCN (30 cm³). Addition of Et_2O (20 cm³) yielded a white solid (43 mg, 57%) (Found: C, 35.7; H, 3.0. $C_{31}H_{34}Au_2Cl_2P_2S_2$ requires C, 36.1; H, 3.2%). FAB mass spectrum: m/z = 961 and 729; calc. 961 for $[Au_2(RSC_3H_6SR)^{35}Cl]^+$ and 729 for $[Au(RSC_3H_6SR)]^+$. NMR (300 K): $^{31}P-\{^1H\}$ (145.8 MHz, CH_2Cl_2–$CDCl_3$), δ 24.9 (s); ^1H (300 MHz, $CDCl_3$), δ 8.78–7.37 (m, 20 H, Ph), 2.95–2.72 (m, 12 H, CH_2) and 1.95 (t, 2 H, CH_2). IR (CsI disc): 2922m, 2851w, 1969w, 1585w, 1432m, 1382w, 1309w, 1259w, 1103m, 997w, 802w, 744w, 692m, 521m, 487w and 326vw cm⁻¹. Conductivity measurement (CH_2Cl_2 solution): non-electrolyte.

(e) **[Au₂(RSC₂H₄SR)₂]Cl₂.** The compound RSC_2H_4SR (75

mg, 0.14 mmol) was dissolved in degassed CH_2Cl_2 (20 cm³) and [AuCl(tht)] (48 mg, 0.15 mmol) was added in one portion. The reaction mixture was stirred for 30 min before the volume was reduced to 2 cm³ in vacuo. Addition of Et_2O (15 cm³) yielded a white solid (71 mg, 68%) (Found: C, 47.8; H, 4.2. $C_{60}H_{64}Au_2Cl_2P_4S_4$ requires C, 48.0; H, 4.3%). FAB mass spectrum: m/z = 715; calc. 715 for $[Au(RSC_2H_4SR)]^+$. NMR (300 K): $^{31}P-\{^1H\}$ (145.8 MHz, CH_2Cl_2–$CDCl_3$), δ 33.0 (s); ^1H (300 MHz, $CDCl_3$), δ 7.95–7.40 (m, 20 H, Ph) and 3.30–2.65 (br m, 12 H, CH_2). IR (CsI disc): 3047m, 2903w, 1568w, 1481m, 1432s, 1309w, 1260w, 1182m, 1158m, 1101s, 1026m, 997m, 894w, 834m, 743m, 693s, 598w, 513s and 482m cm⁻¹. Conductivity: Λ_M = 17.0 (CH_2Cl_2 solution), 65.0 Ω^{-1} cm² mol⁻¹ (MeNO₂ solution).

X-Ray crystallography

Details of the crystallographic data collection and refinement parameters are given in Table 4 for the three structures. The crystals were grown by layering solutions of the complexes with diethyl ether {or pentane for $[Au_2(RSC_2H_4SR)_2]Cl_2$·4CH₂Cl₂} at −15 °C. In each case the selected crystal was coated with mineral oil and mounted on a glass fibre. Data collection used a Rigaku AFC7S four-circle diffractometer equipped with an Oxford Cryostreams low-temperature attachment operating at 150 K, graphite-monochromated Mo-Kα X-radiation (λ = 0.710 73 Å) and ω–2θ scans. The intensities of three standard reflections were measured after every 150 data. No significant crystal decay or movement was observed. As there were no identifiable faces, the data for each crystal were corrected for absorption using ψ scans. The structures were solved by direct methods[15] and developed by iterative cycles of full-matrix least-squares refinement (on F) and Fourier-difference syntheses.[16] The weighting scheme w^{-1} = $\sigma^2(F)$ gave satisfactory agreement analyses in each case.

[Au(RSC₂H₄SR)]PF₆. The asymmetric unit contained a discrete, ordered $[Au(RSC_2H_4SR)]^+$ cation and PF_6^- anion. The phenyl rings were refined as rigid groups with the C atoms in each ring having common isotropic thermal parameters. The Au, P, S and F atoms were refined anisotropically and the H atoms were included in fixed, calculated positions. The absolute configuration of the structure was checked by inverting the coordinates and re-refining the structure to convergence. The hand chosen gave significantly smaller R and R' values and

Table 7 Fractional atomic coordinates for [Au$_2$(RSC$_2$H$_4$SR)$_2$]Cl$_2$·4CH$_2$Cl$_2$

Atom	x	y	z	Atom	x	y	z
Au	0.383 01(1)	0.024 60(2)	0.147 75(1)	C(12)	0.297 6(3)	−0.079 7(4)	−0.001 9(3)
Cl(1)	0.50	0.013 8(1)	0.25	C(13)	0.376 5(3)	−0.182 0(4)	0.177 3(3)
Cl(2)	1.00	0.003 1(1)	0.25	C(14)	0.412 7(3)	−0.252 1(4)	0.192 7(3)
Cl(3)	−0.109 0(2)	0.035 4(3)	0.032 0(2)	C(15)	0.403 9(3)	−0.304 8(4)	0.239 7(4)
Cl(4)	0.004 0(2)	0.136 1(2)	0.074 3(1)	C(16)	0.359 3(3)	−0.287 0(4)	0.273 0(3)
Cl(5)	0.814 16(10)	0.091 3(1)	0.720 1(1)	C(17)	0.323 0(3)	−0.218 1(4)	0.257 7(3)
Cl(6)	0.848 3(1)	0.025 3(2)	0.853 0(1)	C(18)	0.331 3(3)	−0.166 1(4)	0.210 2(3)
S(1)	0.570 14(8)	−0.081 6(1)	0.063 06(8)	C(19)	0.297 5(3)	0.202 0(4)	0.112 5(3)
S(2)	0.684 24(8)	0.064 6(1)	0.228 04(8)	C(20)	0.245 1(3)	0.149 5(4)	0.099 1(3)
P(1)	0.389 80(8)	−0.108 0(1)	0.118 63(8)	C(21)	0.183 5(3)	0.176 0(5)	0.067 5(3)
P(2)	0.375 69(8)	0.162 76(10)	0.158 11(8)	C(22)	0.173 6(4)	0.255 5(3)	0.049 1(3)
C(1)	0.471 1(3)	−0.127 5(4)	0.114 9(3)	C(23)	0.224 4(4)	0.308 4(5)	0.061 2(3)
C(2)	0.490 7(3)	−0.065 0(4)	0.072 3(3)	C(24)	0.286 8(3)	0.282 2(4)	0.092 6(3)
C(3)	0.620 8(3)	−0.050 7(4)	0.142 9(3)	C(25)	0.437 5(3)	0.217 9(4)	0.134 3(3)
C(4)	0.621 6(3)	0.040 2(4)	0.154 2(3)	C(26)	0.457 0(3)	0.295 4(4)	0.157 7(3)
C(5)	0.670 2(3)	0.171 5(4)	0.230 8(3)	C(27)	0.506 2(3)	0.333 6(4)	0.139 3(3)
C(6)	0.385 7(3)	0.194 5(4)	0.242 9(3)	C(28)	0.535 9(3)	0.296 0(4)	0.098 0(3)
C(7)	0.338 4(3)	−0.136 5(4)	0.036 4(3)	C(29)	0.516 5(3)	0.219 8(4)	0.074 7(3)
C(8)	0.340 7(3)	−0.213 1(4)	0.011 6(3)	C(30)	0.467 9(3)	0.181 2(4)	0.092 6(3)
C(9)	0.302 4(3)	−0.232 3(5)	−0.051 0(4)	C(31)	−0.032 8(6)	0.047 0(7)	0.079 4(5)
C(10)	0.261 9(3)	−0.175 8(5)	−0.089 2(3)	C(32)	0.846 6(3)	0.008 8(4)	0.770 6(4)
C(11)	0.259 3(3)	−0.100 1(5)	−0.064 8(3)				

smaller estimated standard deviations (e.s.d.s) on the atomic coordinates. Fractional atomic coordinates are listed in Table 5.

[Au(RSC$_3$H$_6$SR)]PF$_6$. The asymmetric unit contained a discrete, ordered [Au(RSC$_3$H$_6$SR)]$^+$ cation and PF$_6^-$ anion. The phenyl rings were refined as rigid groups. The Au, P, S, F and H atoms were treated as above. The final ΔF synthesis showed the maximum residual electron-density peak of 2.2 e Å^{-3} (within 1 Å of the Au atom and are therefore probably due to the absorption effects of the heavy atom: an attempt to apply an alternative absorption correction using DIFABS^{17} did not significantly improve the structure). Fractional atomic coordinates are listed in Table 6.

[Au$_2$(RSC$_2$H$_4$SR)$_2$]Cl$_2$·4CH$_2$Cl$_2$. The asymmetric unit contained one gold atom and two half RSC$_2$H$_4$SR ligands {related by a crystallographic two-fold operation (0, y, 0.25) to give the complete [Au$_2$(RSC$_2$H$_4$SR)$_2$]$^{2+}$ cation}, two half-occupied Cl$^-$ ions [occupying two-fold sites at (0, y, 0.25) and (0.5, y, 0.25)] and two CH$_2$Cl$_2$ solvent molecules (occupying general positions). All non-H atoms were refined anisotropically and the H atoms were included in fixed, calculated positions. The final ΔF synthesis showed one peak of 1.71 e Å^{-3} [0.47 Å from Cl(1)]. In view of the residual peak very close by, we felt that it was necessary to confirm that our assignment for Cl(1) was correct (it would have to be a monoanion in order to balance the charges). This was achieved both through a Fuchsin dye test for trace amounts of Br$^-$ in the presence of Cl$^-$ which proved negative on crystals from the same batch of sample (sensitivity 3 µg Br$^-$)^{18} and also through attempts to refine Cl(1) as a bromine atom which gave a much poorer model (an unacceptable isotropic thermal parameter, higher R factors and e.s.d.s). Fractional atomic coordinates are listed in Table 7.

Complete atomic coordinates, thermal parameters and bond lengths and angles for the three structures have been deposited at the Cambridge Crystallographic Data Centre. See Instructions for Authors, *J. Chem. Soc., Dalton Trans.*, 1996, Issue 1.

References

1 See, for examples, S. J. Berners-Price, R. K. Johnson, C. K. Mirabelli, L. F. Faucette, F. L. McCabe and P. J. Sadler, *Inorg. Chem.*, 1987, **26**, 3383; S. J. Berners-Price and P. J. Sadler, *Chem. Ber.*, 1986, **46**, 541; S. J. Berners-Price, G. R. Girard, D. T. Hill, B. M. Sutton, P. S. Jarret, L. F. Faucette, R. K. Johnson, C. K. Mirabelli and P. J. Sadler, *J. Med. Chem.*, 1990, **33**, 1386.

2 R. V. Parish and S. M. Cottrill, *Gold Bull.*, 1987, **20**, 3; S. T. Cooke, R. M. Snyder, T. R. Butt, F. J. Ecker, H. S. Allaudeen, B. Monia and C. K. Mirabelli, *Biochem. Pharmacol.*, 1980, **35**, 3423.

3 See, for example, S. G. Murray and F. R. Hartley, *Chem. Rev.*, 1981, **81**, 365 and refs. therein; K. C. Dash and H. Schmidbaur, *Chem. Ber.*, 1973, **106**, 1221; G. W. A. Fowles, D. A. Rice and M. J. Riedl, *J. Less-Common Met.*, 1973, **32**, 379; M. G. B. Drew and M. J. Riedl, *J. Chem. Soc., Dalton Trans.*, 1973, 52; J. Strahle, W. Hiller and W. Conzelmann, *Z. Naturforsch., Teil B*, 1984, **39**, 538; P. G. Jones and J. Lautner, *Acta Crystallogr., Sect. C*, 1988, **44**, 2089; D. Parker, P. S. Roy, G. Ferguson and M. M. Hunt, *Inorg. Chim. Acta*, 1989, **155**, 227.

4 A. J. Blake, R. O. Gould, J. A. Greig, A. J. Holder, T. I. Hyde and M. Schroder, *J. Chem. Soc., Chem. Commun.*, 1989, 876; A. J. Blake, J. A. Greig, A. J. Holder, T. I. Hyde, A. Taylor and M. Schroder, *Angew. Chem., Int. Ed. Engl.*, 1990, **29**, 197; A. J. Blake, R. O. Gould, C. Radek, G. Reid, A. Taylor and M. Schroder, *The Chemistry of the Copper and Zinc Triads*, eds. A. J. Welch and S. K. Chapman, The Royal Society of Chemistry, London, 1993, p. 95; A. J. Blake, A. Taylor and M. Schroder, *J. Chem. Soc., Chem. Commun.*, 1993, 1097.

5 N. R. Champness, C. S. Frampton, G. Reid and D. A. Tocher, *J. Chem. Soc., Dalton Trans.*, 1994, 3031.

6 N. R. Champness, R. J. Forder, C. S. Frampton and G. Reid, *J. Chem. Soc., Dalton Trans.*, preceding paper.

7 C. L. Doel, C. S. Frampton, A. M. Gibson and G. Reid, *Polyhedron*, 1995, **14**, 3139.

8 J. J. Guy, P. G. Jones and G. M. Sheldrick, *Acta Crystallogr., Sect. B*, 1976, **32**, 1937.

9 J. A. Muir, M. M. Muir and E. Lorca, *Acta Crystallogr., Sect. B*, 1980, **38**, 931.

10 S. J. Berners-Price, M. A. Mazid and P. J. Sadler, *J. Chem. Soc., Dalton Trans.*, 1984, 969; D. S. Eggleston, D. F. Chodosh, G. R. Girard and D. T. Hill, *Inorg. Chim. Acta*, 1985, **108**, 221.

11 W. J. Geary, *Coord. Chem. Rev.*, 1971, **7**, 81.

12 A. L. Airey, G. F. Swiegers, A. C. Willis and S. B. Wild, *J. Chem. Soc., Chem. Commun.*, 1995, 695.

13 R. Usòn, A. Laguna and J. Vincente, *J. Organomet. Chem.*, 1977, **131**, 471.

14 Y.-M. Hsiao, S. S. Chojnacki, P. Hinton, J. H. Reibenspies and M. Y. Darensbourg, *Organometallics*, 1993, **12**, 870.

15 SHELXS 86, Program for crystal structure solution, G. M. Sheldrick, *Acta Crystallogr., Sect. A*, 1990, **46**, 467.

16 TEXSAN Crystal Structure Analysis Package, Molecular Structure Corporation, Houston, TX, 1992.

17 N. Walker and D. Stuart, *Acta Crystallogr., Sect. A*, 1983, **39**, 158.

18 A. I. Vogel, *A Textbook of Macro and Semimicro Qualitative Inorganic Analysis*, 4th edn., Longmans, London, 1960, p. 357.